Theoretical description of the electrical conduction in atomic and molecular junctions

J C Cuevas[1], J Heurich[1], F Pauly[1], W Wenzel[2] and Gerd Schön[1,2]

[1] Institut für Theoretische Festkörperphysik, Universität Karlsruhe, 76128 Karlsruhe, Germany
[2] Forschungszentrum Karlsruhe, Institut für Nanotechnologie, 76021 Karlsruhe, Germany

Abstract
We present a theoretical analysis of the electronic transport through atomic and molecular junctions. The main goal of this work is to show how the electronic structure of single atoms and molecules controls the macroscopic electrical properties of the circuits in which they are used as building blocks. In particular, we review our work on three basic problems that have received special experimental attention in recent years: (i) the conductance of a single-atom contact, (ii) the conductance of a hydrogen molecule and (iii) the current through single organic molecules.

The recent advances in nanofabrication have triggered the hope that electronic devices can be shrunk down to the single-molecule scale [1, 2]. In fact, it has been already shown that single molecules can perform functions analogous to those of the key components of today's microelectronics, such as switches [3–5], rectifiers [6] and electronic mixers [7]. In view of these achievements one can get the impression that *molecular electronics* is about to replace the traditional technology of microelectronics based on silicon. However, the future of this new field depends crucially on our understanding of the transport mechanisms in single-molecule junctions, and at this stage there are still very basic problems which remain unsolved. Thus, for instance, from the experimental side it is difficult to achieve an unambiguous contact to a single molecule [8], and in many cases the measurements are not reproducible. On the theoretical side the situation is even more unsatisfactory. In this field there are notorious differences between different theories, not to mention the discrepancies between theory and experiment.

In this context it is worth revising some of the emerging concepts in molecular electronics. There are many different mechanisms that in principle can control the current at the single-molecule scale. However, in addition to generic principles of nanoscale physics, e.g. Coulomb blockade, the chemistry and geometry of the molecular junction emerge as the fundamental tunable characteristics of molecular circuits. In this review we shall summarize our efforts to understand the electronic transport in atomic and molecular junctions. Our main goal is to show how the electronic structure of individual atoms and molecules determines the macroscopic electrical properties of the circuits in which they are embedded. Making use of a combination of quantum chemistry methods and non-equilibrium Green function techniques, we shall describe the electronic transport in some of the most basic situations. To be precise, we study three examples of special experimental interest: (i) the conductance of single-atom contacts, (ii) the conductance of a hydrogen molecule and (iii) the current through simple organic molecules.

The rest of the review is organized as follows. In section 1 we shall describe the theoretical formalism used to compute the different results in this work. Section 2 is devoted to the analysis of the conductance of single-atom contacts. In section 3 we study the conductance of a hydrogen molecule. In section 4 we shall investigate the current through simple organic molecules. Finally, in section 5 we present a brief summary of the main conclusions of this work. In every section one can find a brief introduction to the corresponding topic. Those impatient readers who want to get a quick idea about the content of this work are recommended to jump directly to this last section.

1. Theoretical approach

In order to analyse the electrical current in atomic and molecular junctions we use a combination of *ab initio* quantum chemistry calculations and non-equilibrium Green function techniques. Such a combination allows us to bridge traditional concepts of molecular physics and mesoscopic physics, and in particular it allows us to establish the relation between the electronic structure of single atoms and molecules and the transport properties of the macroscopic circuits in which they are integrated. This type of approach has become quite popular and nowadays it is used by many authors [9–20]. The methods only differ in their level of sophistication and in some technical details in their practical implementation. In the rest of this section we briefly describe the approach used to compute the results presented in this work.

Our approach starts with a description of the electronic structure of a molecular junction, like the one shown schematically in figure 1(a), which is based on the following Hamiltonian:

$$\hat{H} = \hat{H}_L + \hat{H}_R + \hat{H}_C + \hat{V}. \quad (1)$$

Here, $\hat{H}_C$ describes the 'central cluster' of the system, which contains the molecule plus part of the leads (see figure 1), $\hat{H}_{L,R}$ describe the left and right electrode, respectively, and $\hat{V}$ gives the coupling between the electrodes and the central cluster. Since the current is mainly controlled by the narrowest part of the system, the electronic structure of the central cluster must be resolved in detail. We do this within the density functional theory (DFT) approximation [21]. The left and right reservoirs are modelled as two perfect crystals of the corresponding metal using the tight-binding parametrization of [22, 23]. The inclusion of part of the leads in the *ab initio* calculation is an important ingredient that ensures the correct description of the molecule–electrode coupling, the charge transfer between the molecule and the leads and therefore the lineup of the molecular levels relative to the metal Fermi level [24]. The Fermi level is set naturally by the highest occupied molecular orbital (HOMO) for a sufficiently large number of metallic atoms in the central cluster.

In order to obtain the current for a constant bias voltage, V, between the leads, we make use of non-equilibrium Green function techniques. Since the Hamiltonian of equation (1) does not contain inelastic interactions, one can show that the current adopts the usual form of the Landauer formula (for a detailed derivation of the following expressions see [25, 26]):

$$I = \frac{2e}{h}\int_{-\infty}^{\infty} \mathrm{d}\epsilon\ \mathrm{Tr}\{\hat{t}\hat{t}^{\dagger}\}[f(\epsilon - eV/2) - f(\epsilon + eV/2)], \quad (2)$$

where f is the Fermi function and $\hat{t}$ is the energy- and voltage-dependent transmission matrix given by

$$\hat{t}(\epsilon, V) = 2\hat{\Gamma}_L^{1/2}(\epsilon - eV/2)\hat{G}_C^r(\epsilon, V)\hat{\Gamma}_R^{1/2}(\epsilon + eV/2). \quad (3)$$

The scattering rate matrices are given by $\hat{\Gamma}_{L,R} = \mathrm{Im}(\hat{\Sigma}_{L,R})$, where $\hat{\Sigma}_{L,R}$ are the self-energies which contain the information of the electronic structure of the leads and their coupling to the central cluster. They can be expressed as $\hat{\Sigma}_{L,R}(\epsilon) = \hat{v}_{CL,R} g_{L,R}(\epsilon)\hat{v}_{L,RC}$, $\hat{v}$ being the hopping matrix which describes the connection between the central cluster and the leads. $g_{L,R}$ are the Green functions of the uncoupled leads, which we assume to be the bulk Green functions of the corresponding metal. Finally, the central cluster Green functions are given by

$$\hat{G}_C(\epsilon, V) = [\epsilon\hat{1} - \hat{H}_C - \hat{\Sigma}_L(\epsilon - eV/2) - \hat{\Sigma}_R(\epsilon + eV/2)]^{-1}. \quad (4)$$

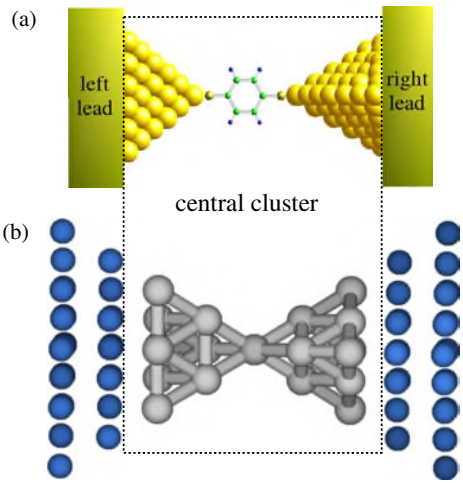

Figure 1. (a) Schematic representation of a single-molecule contact. Notice that the 'central cluster' consists of the molecule plus part of the metallic leads. (b) Single-atom contact consisting of a fcc structure with bulk interatomic distances grown along the (111) direction. The blue atoms represent the bulk atoms used to model the reservoirs.

In this work we shall mostly concentrate on the analysis of the transport in the linear regime, in which the low temperature conductance is given by $G = G_0\,\mathrm{Tr}\{\hat{t}\hat{t}^{\dagger}\} = G_0\sum_i T_i$, where $G_0 = 2e^2/h$ is the quantum of conductance and the T_i's are the transmission eigenvalues at the Fermi energy E_F. As will become clear in the next sections, the analysis of the current in terms of *conduction channels*, defined as eigenfunctions of $\hat{t}\hat{t}^{\dagger}$, provides a deep understanding of the electronic transport.

In the different expressions described above we have assumed that the local basis set in which the Hamiltonian matrix elements are calculated is orthogonal. However, in quantum chemistry it is convenient to use non-orthogonal basis sets. In this case it is straightforward to implement the overlap matrix into these formulae via a Löwdin transformation (see, e.g., [27]).

Finally, it is important to remark on some of the limitations of this type of approach. First of all, it is a mean field approach and therefore strong correlation effects, like Coulomb blockade or the Kondo effect, are out of its scope. Furthermore, in this framework we only describe the current due to elastic processes and the possible influence of inelastic mechanisms, such as molecular vibrations or rotations, is not taken into account.

2. The conductance of a single-atom contact

What determines the electrical conduction in the simplest imaginable circuit, namely a one-atom contact between two metallic banks? Or, in other words, what is the conductance of a single atom? This is the basic question which we address

theoretically in this section. Our main goal here is to show that the properties of such a contact are mainly determined by the nature of the atom.

Using simple experimental techniques such as the scanning tunnelling microscope (STM) or the so-called mechanically controllable break junctions (MCB) it is possible to gently break a metallic contact to form a wire of atomic dimensions. Indeed, the diameter of these nanowires can be easily reduced to a single atom. These atomic-size contacts have been extensively studied in the last decade and they have turned out be an ideal test bed for concepts from mesoscopic physics. The activity in this field has been recently summarized in an excellent review by Agraït *et al* [28] and we refer the reader to this work for more details about these systems.

During the breaking of one of these nanowires the conductance decreases in steps until the contact breaks. The step heights are of the order of G_0. This fact led many authors to interpret this phenomenon as conductance quantization, in analogy with the case of ballistic point contacts in semiconductor heterostructures [29, 30]. However, in the case of metallic atomic-size contacts the conductance plateaux are different for each individual opening of the contact. Moreover, it has been shown that the value of the conductance, the length of the plateaux and the behaviour within the plateaux are characteristic of each metal. In an attempt to study more systematically the occurrence or not of the conductance quantization, histograms of conductance values were introduced, constructed from a large value of conductance curves. These demonstrated that, in some metals, such as gold or sodium, the conductance has a certain preference for multiples of G_0, while for many other materials there is no signature of quantization. The interpretation of these histograms has given rise to a lively debate, which was largely clarified with the help of the breakthrough of Scheer *et al* [31]. These authors demonstrated that the set of transmission coefficients T_i is amenable to measurement in the case of superconducting metals. Since then other techniques, such as shot noise [32], conductance fluctuations [33] and thermopower [34], have also been used to probe the individual conduction channels. In their original paper Scheer and co-workers analysed Al atomic-size contacts using microfabricated breakjunctions. They showed that, in the last plateau before breaking the contact, where typically $G < G_0$, three channels contribute significantly (more than 1% of the total transmission) to the conductance. Several fundamental questions immediately arose from this work: what is the microscopic origin of the conducting channels in a metallic contact? What properties determine the number and transmission of the conducting modes in a given metallic atomic-size contact? The most satisfactory answer to these questions has been given by Cuevas and co-workers [35–37] within the framework of a tight-binding model. The rest of this section is devoted to reviewing these ideas.

We analyse now the current through a single-atom contact at a simple level making use of the orthogonal tight-binding parametrization of [22], which is known to reproduce the electronic structure of bulk materials. This means that we use the bulk hoppings to construct also the Hamiltonian matrix elements of the atomic constrictions (H_C in equation (1)). Here the basis is formed by nine orbitals, namely the s, p and d orbitals which give the main contribution to the bulk density of states (DOS) around the Fermi energy. It is important to remark that we include hopping elements up to second neighbours. In an atomic contact the local environment in the neck region can be very different to that of the bulk material and therefore the use of bulk parameters in the Hamiltonian requires some justification. In the first place, the inhomogeneity of the contact geometry can produce large deviations from the approximate local charge neutrality that typical metallic elements must exhibit. Within the tight-binding approximation we correct this effect by imposing local charge neutrality through a self-consistent variation of the diagonal Hamiltonian matrix elements. This self-consistency in the neck region turns out to be crucial for the correct determination of the conduction channels. Regarding the hopping elements, although we consider them as being equal to the bulk values in order to represent a neck geometry with bulk interatomic distances; one can show that the main results are robust with respect to fluctuations in the hopping elements induced by disorder in the atomic positions (see [35] for more details).

In this work we analyse the following four metals: Au, Al, Pb and Rh. We have chosen these materials to cover a broad range of valences and orbital structures. As a reference the bulk DOS of these metals is shown in figure 2. We have computed the transmission and its decomposition into channels for the structure shown in figure 1(b) and the results can be seen in figure 3. The main findings are the following. The Au contact has a conductance close to G_0, which is largely dominated by a single channel. In the case of Al the total transmission at the Fermi energy is also close to 1, but there are three channels with a significant contribution. In the Pb contact the transmission is also formed by three channels, but the conductance has a value of $2.34G_0$. Finally, in the case of the transition metal Rh the conductance is composed of five channels, giving a total transmission of 1.68.

Let us now discuss the origin of these results. Although the linear conductance is only determined by the transmission at the Fermi energy, it is very illustrative to have a look at the whole energy range considered in our calculations. As can be seen in figure 3, irrespective of the material, one can roughly identify three different energy regions according to the number of channels. There is a region with a single transmission channel, which corresponds roughly to the region in which the s band dominates the bulk DOS. There is a region with three channels which can be associated with the p band. Finally, there is a region with approximately five channels located in the energy window corresponding to the bulk d band. Of course, the actual conductance of the different metals depends on the position of the Fermi energy, which in turn is determined by the charge neutrality condition. In other words, the conductance of a particular metallic one-atom contact depends on the number of valence electrons, i.e. on the chemical valence. Following [35], in order to understand what controls the number of channels we now make two assumptions that simplify the model. First, we consider only nearest-neighbour interactions. Second, we reduce the size of the basis, N_{orb}, in such a way that we only consider the s band for monovalent metals such as the alkali and noble metals, the s and p bands for metals such as Al or Pb, and the s and d bands for transition metals. One can easily check that these

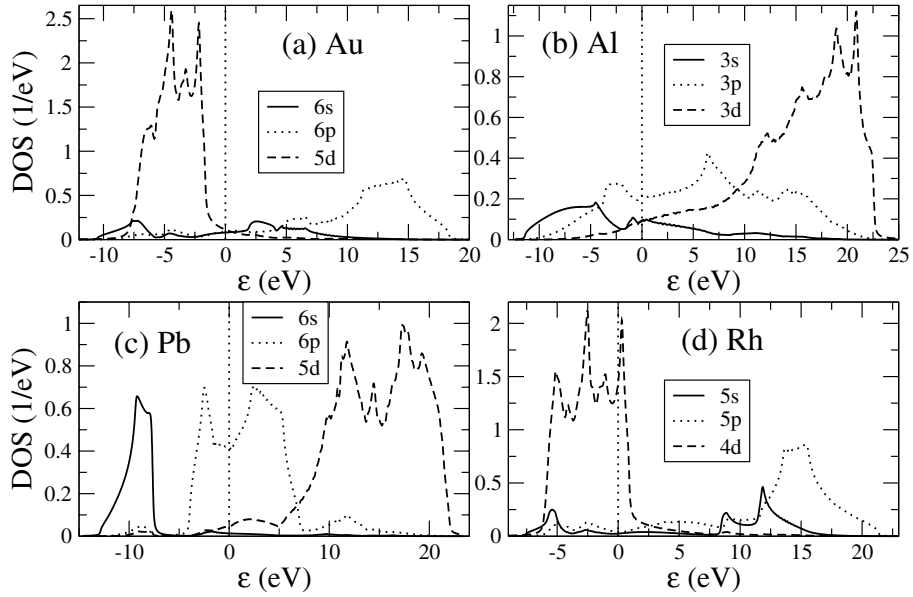

Figure 2. Bulk DOS as a function of energy for Au, Al, Pb and Rh. The DOS is projected into the s, p and d bands around the Fermi energy, which is set to zero and is indicated with a vertical dotted line.

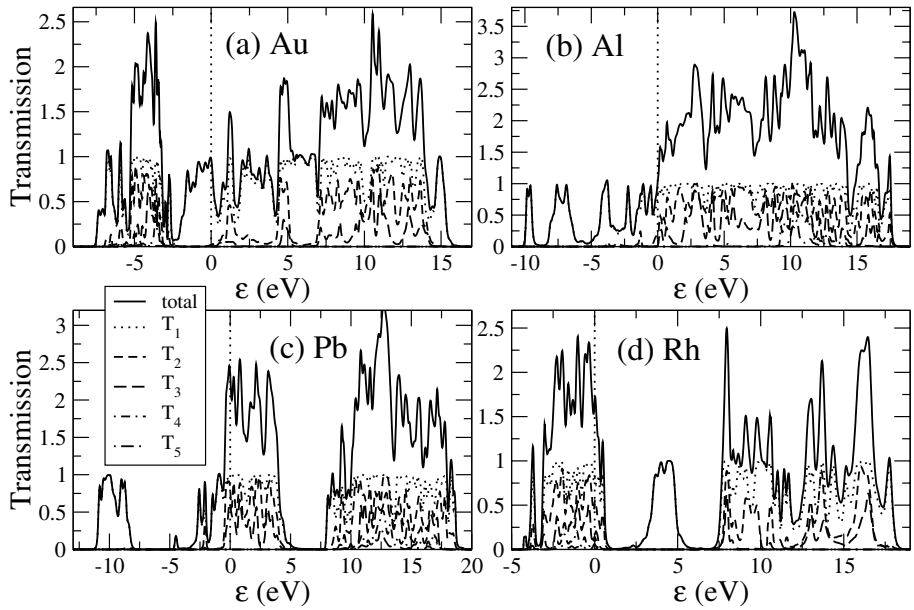

Figure 3. Transmission and channel decomposition as a function of energy of the structure shown in figure 1(b) for four metals: Au, Al, Pb and Rh. The Fermi energy is set to zero and is indicated with a vertical dotted line. For simplicity the channels are ordered according to the transmission value, and not according to their character. The total transmission and the transmission coefficients at the Fermi energy are the following. (a) Au: $T_{total} = 0.97$, $T_1 = 0.95$, and $T_2 = 0.02$. (b) Al: $T_{total} = 1.046$, $T_1 = 0.817$, $T_2 = 0.208$, $T_3 = 0.019$, $T_4 = 0.002$. (c) Pb: $T_{total} = 2.345$, $T_1 = 0.959$, $T_2 = 0.798$, $T_3 = 0.588$, $T_4 = 2 \times 10^{-5}$. (d) Rh: $T_{total} = 1.680$, $T_1 = 0.784$, $T_2 = 0.523$, $T_3 = 0.167$, $T_4 = 0.142$, $T_5 = 0.060$, $T_6 = 10^{-4}$.

two approximations give reasonable results. The maximum number of channels is determined by the dimension of $\hat{t}\hat{t}^{\dagger}$, which can be arbitrarily large, depending on the size of the central cluster. However, the actual number of conducting channels (those with a nonvanishing transmission eigenvalue T_i) are limited by the number of orbitals in the narrowest section of the neck (N_{orb} when having a single-atom contact). This fact can be shown by the following simple argument. As the division between central cluster and leads is somewhat arbitrary, one could always redefine the leads for the geometry of figure 1(b) in such a way that the new central cluster consists of only the central atom. Then, the new scattering rate matrices $\hat{\Gamma}_{L,R}$ have a dimension of just N_{orb} and the new transmission matrix would only admit N_{orb} eigenmodes. Current conservation along each conducting channel ensures that the nonvanishing eigenvalues T_i are the same, no matter where the transmission matrix is calculated.

The above simple argument already gives us a rule of thumb to estimate the maximum number of relevant conduction channels in a one-atom contact. Thus, for monovalent metals

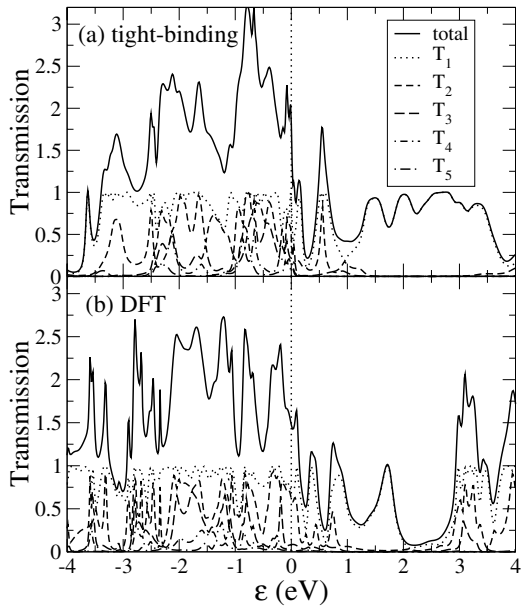

Figure 4. Transmission and channel decomposition as a function of the energy of the structure shown in figure 1(b) for Pt. Panel (a) corresponds to the tight-binding calculation and panel (b) to the DFT calculation. The Fermi energy is set to zero and is indicated with a vertical dotted line.

such as the noble and alkali metals, one expects a single channel. For an sp-like metal like Al or Pb, this number should be typically four, while for a transition metal like Rh (having a negligible weight of p orbitals at E_F) this number would be of the order of six. Indeed, comparing the results of figure 3 and the estimation of this simple rule we see that there is a slight deviation in the case of the sp-like metals, where the actual number of channels is three instead of four, and in the case of the transition metal Rh where there are five channels instead of six. One is tempted to explain these discrepancies by saying that one can further reduce the size of the basis by removing the s band. However, in general this is not a good approximation. For instance, while in the case of Pb this might be reasonable, due to the large separation between the s level and the Fermi energy, in the case of Al it cannot be justified, since the Fermi level indeed lies closer to the s level. On the other hand, such an approximation would not explain why there are no energy regions with four or six transmission channels. The simple rule should be taken as an upper bound. The actual number of conducting channels can be smaller as some of the channels can carry no current due to symmetry considerations. Thus, for instance the analysis of the character of the channels reveals that, in the case of the sp-like metals, the dominant channel is essentially a symmetric combination of the s and p_z orbitals of the central atom, where z is the transport direction. The antisymmetric combination of these two orbitals gives rise to a channel that is closed because it is orthogonal to the incoming metal states. In the same way, in the case of transition metals the s and d_{z^2} orbitals combine to give a widely open channel (symmetric combination) and a closed channel (antisymmetric combination). For a detailed analysis of the character of the channels in a one-atom contact see [26].

So, in short, the analysis above suggests that one can easily estimate the conductance of a single-atom contact just using the information of the number of valence orbitals and the chemical valence. It is worth stressing that the predictions about the number of channels of this tight-binding model have been confirmed so far by all the experiments that have tested the individual channels [31–34, 36]. It is also important to remark that this model explains in a natural way the typical conductance values observed in the different materials. It explains not only the differences between the different classes of metals: monovalent metals (alkali and noble metals), sp-like metals, transition metals, etc, but also the differences between metals of the same class. Thus for instance, within the transition metals the model predicts a simple hierarchy. The highest conductance should be exhibited by V, Nb and Ta (with five valence electrons), since for them the Fermi level lies in the middle of the d band. The conductance, and in particular the transmissions, of the fourth and fifth channels should diminish towards the column of Pd and Pt, since in this case the Fermi level lies in the edge of the d band. Indeed, this is precisely what is observed in the conductance histograms [28]. For the sp-like metals, Pb, Al, Zn, Cd, etc, there is a huge difference between Pb, with four valence electrons, and the other materials, with two or three valence electrons. The conductance of Pb is much higher due to the position of the Fermi energy, well inside the p band.

In recent years several authors have criticized this type of tight-binding calculations and they have emphasized the need to use of *ab initio* methods. We want to stress here that the validity of the approach described above is based on two main facts: first, the separation between the energy bands in a metal is very large, which implies that to identify the relevant orbitals that give rise to the conduction channels is not a difficult task. Second, the charge neutrality is a very good approximation due to the short screening length in a metal. Furthermore, the simplicity of this approach allows us to explore the influence of the geometry, disorder and other ingredients, which is still outside the scope of *ab initio* methods. In order to make our statement more quantitative we show in figure 4 a comparison between the transmission of a Pt contact calculated with the tight-binding approach and with the DFT method described in section 1. The total transmission at the Fermi energy in the case of the tight-binding approach is $T_{total} = 1.82$ and it is composed of five channels in agreement with the simple ideas described above. In the DFT calculations we use the BP86 functional [38] and the basis set of Christiansen *et al* [39]. For the description of the Pt reservoirs we use a basis with the 5d, 6s, 6p orbitals. We find that the HOMO of the central cluster lies at -5.44 eV, which is close to the Pt work function ~ -5.64 eV. The gap between the HOMO and the lowest unoccupied molecular orbital is almost closed (0.12 eV). Thus, we have almost reached bulk properties, which justifies our approach. The total transmission at the Fermi energy is $T_{total} = 1.47$. As in the case of the tight-binding calculations, the transmission is made up of five conduction channels, which is due to the contribution of the Pt d orbitals. This is again in agreement with the simple concepts explained above and it can be taken as a justification of the use of the tight-binding approach.

Although there have been great advances in our understanding of the electrical conduction in atomic-size contacts, there are still some important open problems. For

instance, the origin of the peaks in the conductance histograms is still unclear and it is obvious that a systematic study of the interplay of the mechanical and electrical properties is needed. It would also be important to clarify the relation between the atomistic models, like the one presented here, and the free-electron models, which in some cases predict similar results [40]. It is also desirable to study in more detail other materials like ferromagnetic metals [41–44] and semimetals [45–47].

3. Conductance of a hydrogen molecule

In this section we discuss the electrical conduction through an individual hydrogen molecule. The results described here are based on our recent work of [48]. As we mentioned in the introduction, at this stage of the development of the field of molecular electronics one can hardly find any satisfactory agreement between theory and experiment. In this context the measurement of the conductance of an individual hydrogen molecule reported by Smit *et al* [49] provides a valuable opportunity to analyse the emerging concepts of electrical conduction in single-molecule devices in the perhaps simplest possible system. In [49] it was shown that a single hydrogen molecule can form a stable molecular bridge between platinum contacts. In contrast to results for organic molecules [50–52], this bridge has a conductance close to one quantum unit, carried by a single channel. This result belies the conventional wisdom because the closed-shell configuration of H_2 results in a huge gap between its bonding and antibonding states, making it a perfect candidate for an insulating molecule. Thus, the observations of [49] pose an interesting theoretical challenge and their understanding can help to elucidate some of the basic transport mechanisms at the single-molecule scale.

Before describing the results of our DFT calculations, it is very instructive to discuss our prejudices and naive expectations based on a toy model for the conduction through a hydrogen molecule. We describe H_2 with a two-site tight-binding model, see figure 5(a). In this scheme ϵ_0 represents the 1s energy level of H and t_H is the hopping connecting the H atoms. This hopping is simply related to the splitting between the bonding (ϵ_+) and antibonding state (ϵ_-) of the molecule, namely $\epsilon_\pm = \epsilon_0 \pm t_H$, and its value is ~ -12 eV. The molecule is coupled symmetrically to the leads with a single hopping t. Within this model the total transmission as a function of energy is given by

$$T(\epsilon) = \frac{4\Gamma^2 t_H^2}{[(\epsilon - \tilde{\epsilon}_+)^2 + \Gamma^2][(\epsilon - \tilde{\epsilon}_-)^2 + \Gamma^2]}. \qquad (5)$$

Here, $\tilde{\epsilon}_\pm = \epsilon_0 \pm t_H + t^2\,\mathrm{Re}\{g^a\}$ are the renormalized molecular levels, $g^a(\epsilon)$ being the advanced Green function which describes the local electronic structure of the leads. The scattering rate Γ, which determines the broadening of the molecular levels, is given by $\Gamma(\epsilon) = t^2\,\mathrm{Im}\{g^a\} = \pi t^2 \rho$, where $\rho(\epsilon)$ is the LDOS of the Pt contacts. For the sake of simplicity, let us assume that Γ is energy-independent and that the levels are not renormalized ($\tilde{\epsilon}_\pm = \epsilon_\pm$). In figure 5(b) we show the transmission as a function of energy for different values of Γ in units of t_H. We also show in figure 5(c) the corresponding DOS projected into the bonding and antibonding states of H_2, which

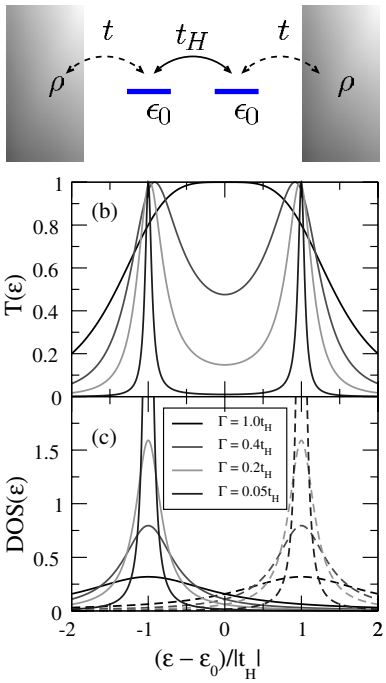

Figure 5. (a) Schematic representation of the toy model described in the text. (b), (c) Transmission and DOS projected into the bonding (full curves) and antibonding (broken curves) states versus energy for different values of the scattering rate Γ.

are given by $\rho_\pm = \Gamma/\pi\{(\epsilon - \tilde{\epsilon}_\pm)^2 + \Gamma^2\}$, respectively. Taking into account the huge value of t_H, one naively expects the curve for $\Gamma = 0.05 t_H$ to represent the relevant situation. Assuming that H_2 remains neutral, the bonding state is occupied by two electrons and $E_F = \epsilon_0$. In this simple picture H_2 would be insulating, in clear disagreement with the observations of [49]. What is missing in this simple picture?

Let us now see if the full DFT calculations can resolve this puzzle. In the last section we showed that a single-atom contact of Pt sustains five conduction channels. Following the experiment of [49], we now study how the presence of H_2 modifies the conduction. Usually the lack of knowledge of the precise geometry of the molecular junction complicates the comparison between theory and experiment. However, in [49] the presence of H_2 was identified by means of the signature of its vibrational modes in the conductance. This information establishes clear constraints on the geometries realized in the experiment. In this sense, we only consider configurations which are compatible with the observed vibrational modes. The most probable configuration is shown in the inset of figure 6, where the H_2 is coupled to a single Pt atom on either side (top position). In this geometry the vibrational mode of the centre of mass motion of H_2, which is the one seen in the experiment, has an energy of 55.6 meV, lying in the range of the experimental values. In figure 6 we also show the transmission and the LDOS projected into the orbitals of one of the H atoms. The total transmission at the Fermi energy is $T_{total} = 0.86$ and it is largely dominated by a single channel, in agreement with experimental results. We would like to draw attention to the following two features in the LDOS:

(i) the bonding state of the molecule appears as a peak at $\sim$6 eV below E_F and the antibonding state, not shown in figure 6, is located at $\sim$18 eV above E_F;

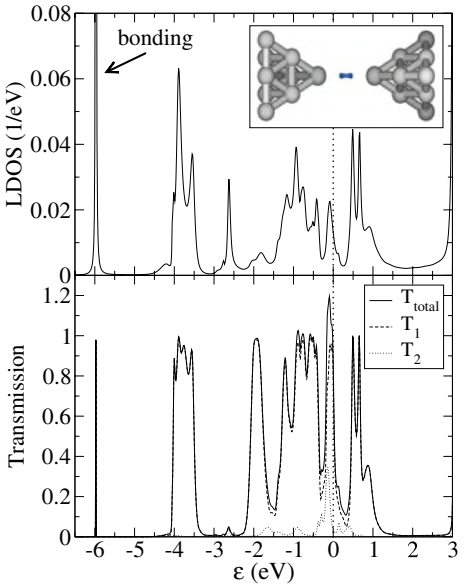

Figure 6. Transmission and LDOS projected onto one of the H atoms as a function of energy for the Pt–H_2–Pt structure, the central cluster of which is shown in the inset. At E_F $T_1 = 0.83$ and $T_2 = 0.03$ the H–H and Pt–H distances are 0.8 and 2.1 Å, respectively. We use the cc-pVDZ basis set for H.

(ii) around the Fermi energy the gap between the molecular states is filled due to the strong hybridization with the Pt leads, which is indeed the mechanism behind the high conductance of this molecule.

How can we understand these results in simple terms? In other words, what ingredients were missing in the toy model presented above? Our DFT calculations indicate that there are two main ingredients missing in this simple argument. First, H forms a bond with Pt by sharing electrons. The DFT calculations show that every H atom donates $\approx 0.12e$ to Pt. This implies that the Fermi level lies closer to the bonding state. With this charge transfer the transmission raises significantly, but it is not yet sufficient to reproduce the DFT results. Thus, a large broadening (Γ) of the bonding state is still needed. As suggested by the DFT calculations, this is provided by the good Pt–H_2 coupling and the large DOS around the Fermi energy coming from the d band of Pt. We test this idea assuming that g^a is the bulk Green function of Pt. The Pt bulk DOS is shown in figure 7(a). We also show in figures 7(b), (c) the transmission and the LDOS projected into one of the H atoms for two values of the coupling to the leads t. One can see that, for realistic values of $t \approx 1$–2 eV, the transmission at E_F can now indeed reach values close to one. Therefore, we conclude that *the high conductance of H_2 is due to the charge transfer between H_2 and the Pt leads and the strong hybridization between the bonding state and the d band of Pt*. This mechanism is not exclusive to Pt and it must also operate in other transition metals, as was shown experimentally for Pd (see [49]).

Let us now address why only a single channel is observed. In view of the model described above a simple explanation could be that all the current flows through the 1s orbital of the closest H atom to the Pt atom. However, the DFT calculations show that, while the Pt–Pt coupling across the

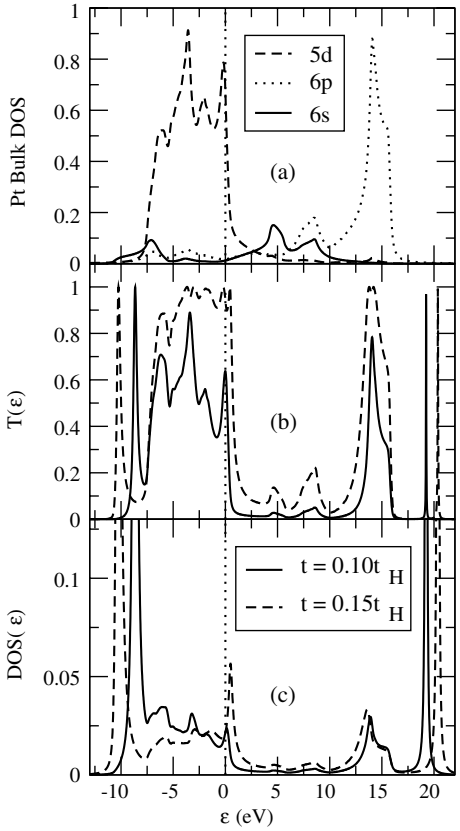

Figure 7. (a) Bulk DOS of the Pt reservoirs. (b), (c) Transmission and LDOS projected onto one of the H atoms for two values of the hopping t, assuming that the leads are modelled by Pt bulk atoms, $t_H = -12$ eV and $\epsilon_0 = 9$ eV. Fermi energy is set to zero and is indicated with a vertical dotted line.

contact is negligible, this is not the case for the Pt and the second H atom. In principle there are two paths for the current, i.e. two channels may occur. Due to the spherical symmetry of the H orbitals there is only coupling to the s and d_{z^2} orbitals of Pt. In addition, the Hamiltonian matrix elements between these orbitals fulfil approximately the condition $H_{1,s}H_{2,d_{z^2}} = H_{1,d_{z^2}}H_{2,s}$, where 1 and 2 stand for the first and second atom of H_2. Therefore, the coupling matrix between the H_2 and the Pt leads is singular, which implies that one of the transmission eigenvalues vanishes. This condition of the hopping matrix elements implies that we can always find a basis in which one of the molecular states is decoupled to the metallic states. So, in short, *one of the molecular states does not couple to the metallic states due to symmetry reasons, reducing the actual number of channels to one*. This phenomenon of symmetry-inhibited modes is well-known in the contexts of light propagation in photonic crystals [53] and sound propagation in periodic structures [54]. This symmetry-induced destructive interference is a unique, but generic feature of the top position and thus a direct indicator of the relative orientation of the H_2 axis to the electrodes.

The above analysis has been performed for a particular geometry and a legitimate question is whether we can be sure that this is the geometry realized in the experiment. In principle, there are other configurations compatible with the vibrational modes analysis. However, based on the channel

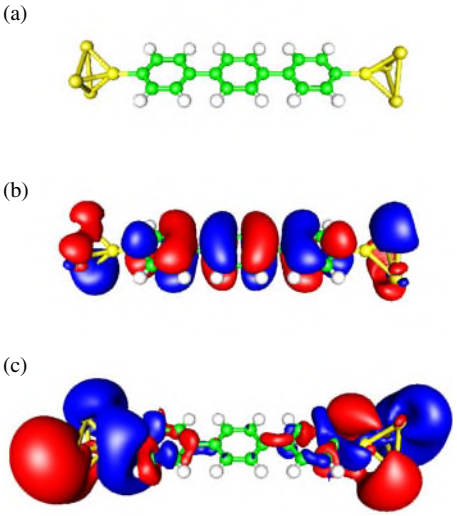

Figure 8. (a) Organic molecule analysed in this work connected to three gold atoms in the hollow position. Colour codes: C (green), H (white), S (yellow), Au (gold). (b) Charge density of the HOMO of the central cluster. (c) Charge density of the LUMO of the central cluster.

analysis performed in the experiment many geometries can be ruled out. For more details about this point we refer the reader to [48].

4. Current through simple organic molecules

Since the pioneering experiment of Reed and co-workers [50] many different organic molecules have been investigated experimentally. Most of these molecules consist of a few benzene rings forming a short wire, which is terminated by thiol groups. This means in practice that the molecules are attached to gold electrodes by means of a stable covalent bond between sulfur and gold. These molecules have usually π delocalized orbitals, which make them in principle ideal building blocks for molecular circuits [55]. There are many different interesting observations, such as negative differential conductance [7], which still, by-and-large, beg theoretical explanation. Another interesting observation is the rectifying behaviour that some molecules exhibit, which is one of the issues that we address below. To be precise, in this section we concentrate ourselves to the answer to the following two questions:

(a) why is the low bias conductance of these molecules much lower than in the hydrogen case?, and
(b) what controls the symmetry of the current–voltage characteristics?

As an example we consider the molecule shown in figure 8(a). It consists of three benzene rings terminated by a thiol group on each side. The S atoms are attached to three Au atoms in the hollow position and the Au–S distance is 2.37 Å. For this molecule, as for many of this type, the work function of gold lies inside the HOMO–LUMO gap, which usually means that there is no significant charge transfer between the metal and the molecule. This is confirmed by the Mulliken population analysis of the central cluster. Thus, the question of whether this molecular junction is highly conductive or not

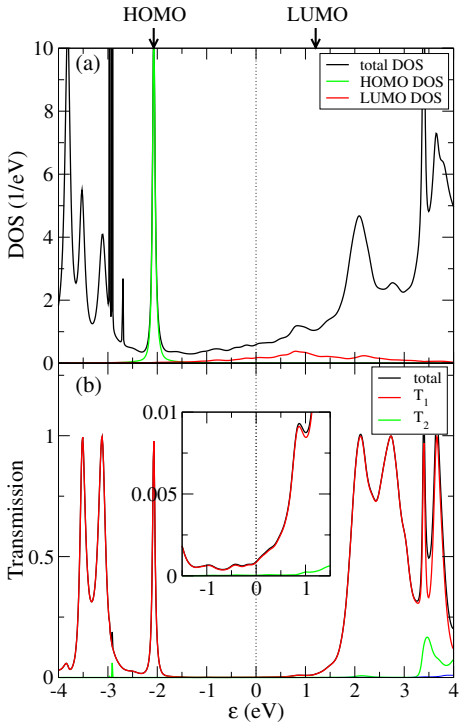

Figure 9. (a) Total DOS and DOS projected into the HOMO and LUMO of the central cluster of the molecular junction shown in figure 8(a). (b) Corresponding zero bias transmission versus energy. The inset show a blow-up of the region around the Fermi energy. Notice that the transmission is largely dominated by a single channel. The Fermi energy has been set to zero.

reduces to the question of whether the coupling to the gold electrodes is strong enough to fill the HOMO–LUMO gap. In the DFT calculation we have used the B3LYP functional [57], the LANL2DZ basis [56] for the atoms of the molecule and the basis set of Christiansen *et al* [39] for the Au atoms. In figure 9 we show both the transmission through the molecule and the DOS of the central cluster. Notice that the transmission at the Fermi energy is 8.2×10^{-4}, which reproduces the general trend observed in these molecules [50–52]. The reason for this low transparency can be understood with the analysis of the DOS. In figure 9(b) we show the DOS projected into the HOMO and LUMO of the central cluster. We see that the HOMO has a width of $\sim$0.3 eV and only its tail reaches the Fermi level. Thus, although this molecular orbital has an extended character, see figure 8(b), it does not give a large contribution to the low bias conductance. The LUMO is broader due to its stronger coupling to the leads, see figure 8(c). However, it does not give either a large contribution at the Fermi energy. So in short, *we can conclude that this molecule does not conduct very well at low bias because its hybridization with metallic electrodes is not strong enough to fill its HOMO–LUMO gap*. Finally, it is important to remark that although we have paid special attention to the contribution of the HOMO and LUMO, there are many other levels close to the Fermi energy, which give at least a similar contribution to the current. This seems to be a common feature of many of these organic molecules [19].

Now we turn to the analysis of the symmetry of the current with respect to voltage inversion. This is an important issue that is intimately related to the possibility that a molecule

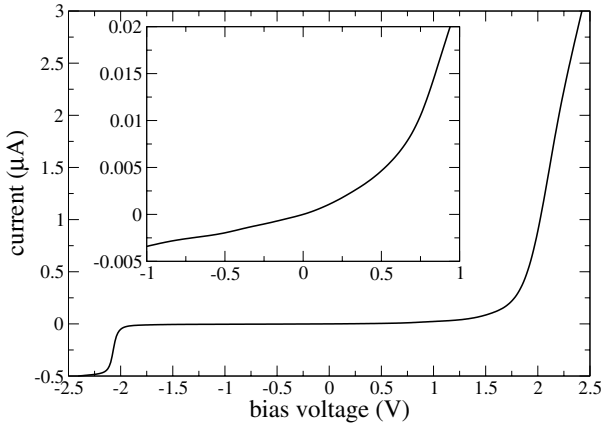

Figure 10. Current versus bias voltage for the molecular junction shown in figure 8(a). The inset shows a blow-up of the region between −1 and 1 V.

behaves as a rectifier. Indeed, this question can be understood in simple terms. The first point that one has to discuss is how the voltage is applied in a real experiment. If the voltage is applied symmetrically, the key issue in order to understand the symmetry is the potential drop along the molecule. If the potential profile is asymmetric, due for instance to an asymmetric coupling to the electrodes, the molecular levels can then line up differently in positive and negative bias, resulting in rectification. This has been nicely explained in [58]. However, in real experiments the voltage is not applied symmetrically, but one of the electrodes is grounded. In this case the key point is the electron–hole asymmetry of the transmission function. Let us explain this point in more detail. At a finite bias there are two main issues that must be considered. First, the position of the molecular levels is altered in principle by the electric field applied across the molecule. Second, strictly speaking the charge density, which is the fundamental quantity in the DFT formalism, should be computed using the non-equilibrium Green functions. In the case of this molecule, we have performed DFT calculations of the spectrum of the central cluster at finite field, and we have obtained that the transmission is not significantly modified. Again, this seems to be a common feature of many of these molecules [15, 19]. Then, assuming that the non-equilibrium occupations are not very different from the equilibrium ones, we can easily calculate the current integrating the zero-bias transmission. Keeping in mind that the chemical potential of one of the electrodes is fixed, the results can be seen in figure 10. Notice that the current is asymmetric even in the case of this spatially symmetric molecule. Indeed, this should be the case for every molecule as long as one explores a sufficiently large voltage range. The large increase of the current at around 2 V is due to the opening of the HOMO and LUMO contributions.

5. Conclusions

In this work we have analysed theoretically the electronic transport through atomic and molecular junctions. The main conclusion is that the set of our results illustrate clearly how the electronic structure of single atoms and molecules determines the macroscopic current of the circuits in which they are used as building blocks. Below, we summarize the main conclusions of the different sections.

Single-atom contacts

The ensemble of the experimental and our theoretical results show unambiguously that the conduction channels in an atomic contact are determined by the orbital electronic structure and the local atomic environment around the neck region. In particular, for the case of one-atom contacts the conduction channels are determined by the chemical nature of the central atom. As a simple rule, we could say that the number of active channels corresponds to the number of valence orbitals of such an atom. Our calculations, in agreement with the experimental results, predict the presence of three conducting channels for sp-like metals, like Al or Pb. For transition metals like Pt, we expect the presence of five conduction modes due to the contribution of d orbitals. In the case of simple metals, such as alkali or noble metals, we expect the presence of a single conducting channel due to the contribution of the s band.

With respect to the conductance quantization, the results shown in this work clearly indicate that this phenomenon does not take place in atomic contacts of sp-like metals or transition metals due to the contribution of p and d orbitals, respectively. As we have shown, in these contacts there are channels with intermediate transmission, even in the absence of disorder. The conductance quantization is thus reserved for simple metals or noble ones, where we have only the contribution of the s band.

Conductance of a hydrogen molecule

We have presented a theory for the conductance of a hydrogen bridge between Pt contacts explaining the experimental observations of [49]. In particular, we have developed

(i) a simple theoretical model to understand the conduction mechanism through the hydrogen bridge which
(ii) we have matched to quantitative DFT calculations of the conductance.

The interplay of these two approaches permits us to identify the two relevant mechanisms that give rise to the large conductance of the hydrogen molecule. First, the catalytic activity of platinum is responsible for a significant charge transfer between H_2 and the Pt contacts, which moves the bonding state of the molecule towards the Fermi energy. Then, the strong hybridization with the d band of the Pt leads provides a large broadening of the bonding state, finally allowing for a high transmission. Additionally, we have shown that, due to the symmetry of its molecular orbitals, H_2 filters out only one of the Pt conduction channels. Our analysis of this ideal test system illustrates that ingredients, such as charge transfer and the electronic structure of the metallic contacts, are essential for the proper description of the electrical conduction in single-molecule devices.

Current through simple organic molecules

We have studied the transport through a simple organic molecule consisting of three benzene rings terminated by thiol groups. We have shown that the low conductance exhibited by

this type of molecule in the low voltage regime is due to the following reason. The hybridization between the molecular orbitals and the metallic states is not strong enough to fill the HOMO–LUMO gap, and the current proceeds then through the tails of the closest levels to the Fermi energy. We have also discussed the origin of the asymmetry in the current–voltage characteristics frequently found in this type of molecule.

Acknowledgments

We are grateful for many stimulating discussions and collaborations with A Martín-Rodero, A Levy Yeyati, E Scheer, C Urbina, D Esteve, M H Devoret, N Agraït, G Rubio, C Untied, B Ludoph, R H M Smit, J M van Ruitenbeek, D Beckmann, M Hettler, M Mayor, H Weber and F Weigend. This work is part of the CFN which is supported by the DFG. JCC acknowledges funding by the EU TMR Network on Dynamics of Nanostructures, and WW by the German National Science Foundation (We 1863/10-1), the BMBF and the von Neumann Institute for Computing.

References

[1] Aviram A and Ratner M (ed) 1998 *Molecular Electronics: Science and Technology* (New York: Annals of the New York Academy of Sciences)
[2] Joachim C, Gimzewski J K and Aviram A 2000 *Nature* **408** 541
Nitzan A 2001 *Annu. Rev. Phys. Chem.* **52** 681
[3] Gao H J *et al* 2000 *Phys. Rev. Lett.* **84** 1780
[4] Collier C P *et al* 1999 *Science* **285** 391
[5] Reed M A *et al* 2001 *Appl. Phys. Lett.* **78** 3735
[6] Metzger R M 1999 *Acc. Chem. Res.* **32** 950
[7] Chen J *et al* 1999 *Science* **286** 1550
[8] Cui X D *et al* 2001 *Science* **294** 571
[9] Joachim C *et al* 1995 *Phys. Rev. Lett.* **74** 2102
[10] Kemp M, Roitberg A, Mujica V, Wanta T and Ratner M A 1996 *J. Phys. Chem.* **100** 8349
Mujica V, Kemp M, Roitberg A and Ratner M A 1996 *J. Chem. Phys.* **104** 7296
[11] Datta S *et al* 1997 *Phys. Rev. Lett.* **79** 2530
[12] Emberly E G and Kirczenow G 1998 *Phys. Rev.* B **58** 10911
[13] Yaliraki S N *et al* 1999 *J. Chem. Phys.* **111** 6997
[14] Di Ventra M, Pantalides S T and Lang N D 2000 *Phys. Rev. Lett.* **84** 979
Di Ventra M *et al* 2001 *Phys. Rev. Lett.* **86** 288
[15] Derosa P A and Seminario J M 2001 *J. Phys. Chem.* **105** 471
Seminario J M and Derosa P A 2001 *J. Am. Chem. Soc.* **123** 12418
[16] Taylor J, Guo H and Wang J 2001 *Phys. Rev.* B **63** 121104
Taylor J, Guo H and Wang J 2001 *Phys. Rev.* B **63** 245407
[17] Palacios J J *et al* 2001 *Phys. Rev.* B **64** 115411
Palacios J J *et al* 2002 *Phys. Rev.* B **66** 035322
[18] Damle P S, Ghosh A W and Datta S 2001 *Phys. Rev.* B **64** 201403
[19] Heurich J *et al* 2002 *Phys. Rev. Lett.* **88** 256803
[20] Brandbyge M *et al* 2002 *Phys. Rev.* B **65** 165401
[21] The DFT calculations have been performed with the code Frisch M J *et al* 1998 *GAUSSIAN98 (Rev. A9)* (Pittsburgh, PA: Gaussian Inc.)
[22] Papaconstantopoulos D A 1986 *Handbook of the Band Structure of Elemental Solids* (New York: Plenum)
[23] Mehl M J and Papaconstantopoulos D A 1996 *Phys. Rev.* B **54** 4519
[24] Xue Y, Datta S and Ratner M A 2001 *J. Chem. Phys.* **115** 4292
[25] Datta S 1995 *Electronic Transport in Mesoscopic Systems* (Cambridge: Cambridge University Press)
[26] Cuevas J C 1999 *PhD Thesis* Universidad Autónoma de Madrid, Madrid, Spain (available in http://www-tfp.physik.uni-karlsruhe.de/cuevas/Publications.html)
[27] Brandbyge M, Kobayashi N and Tsukada M 1999 *Phys. Rev.* B **60** 17064
[28] Agraït N, Levy Yeyati A and van Ruitenbeek J M 2003 *Phys. Rep.* **377** 81
(Agraït N, Levy Yeyati A and van Ruitenbeek J M 2002 *Preprint* cond-mat/0208239)
[29] van Wees B J, van Houten H, Beenakker C W J, Williamson J G, Kouwenhoven L P, van der Marel D and Foxon C T 1988 *Phys. Rev. Lett.* **60** 848
[30] Wharam D A, Thornton T J, Newbury R, Pepper M, Ahmed H, Frost J E F, Hasko D G, Peacock D C, Ritchie D A and Jones G A C 1988 *J. Phys. C: Solid State Phys.* **21** L209
[31] Scheer E, Joyez P, Esteve D, Urbina C and Devoret M H 1997 *Phys. Rev. Lett.* **78** 3535
[32] van den Brom H E and van Ruitenbeek J M 1999 *Phys. Rev. Lett.* **82** 1526
[33] Ludoph B, Devoret M H, Esteve D, Urbina C and van Ruitenbeek J M 1999 *Phys. Rev. Lett.* **82** 1530
[34] Ludoph B and van Ruitenbeek J M 1999 *Phys. Rev.* B **59** 12290
[35] Cuevas J C, Levy Yeyati A and Martín-Rodero A 1998 *Phys. Rev. Lett.* **80** 1066
[36] Scheer E, Agraït N, Cuevas J C, Levy Yeyati A, Ludoph B, Martín-Rodero A, Rubio G, van Ruitenbeek J M and Urbina C 1998 *Nature* **394** 154
[37] Cuevas J C, Levy Yeyati A, Martín-Rodero A, Rubio G, Untiedt C and Agraït N 1998 *Phys. Rev. Lett.* **81** 2990
[38] Becke A D 1988 *Phys. Rev.* A **38** 3098
Perdew J P 1986 *Phys. Rev.* B **33** 8822
[39] Ross R B *et al* 1990 *J. Chem Phys.* **93** 6654
[40] López-Cuidad T *et al* 1999 *Surf. Sci. Lett.* **440** L887
[41] Costa-Krämer J L 1997 *Phys. Rev.* B **55** R4875
[42] García N, Muñoz M and Zhao Y W 1999 *Phys. Rev. Lett.* **82** 2923
[43] Martín-Rodero A, Levy Yeyati A and Cuevas J C 2001 *Physica* C **67** 3535
[44] Viret M, Berger S, Gabureac M, Ott F, Olligs D, Petej I, Gregg J F, Fermon C, Francinet G and Le Goff G 2002 *Phys. Rev.* B **66** 220401
[45] Krans J M and van Ruitenbeek J M 1994 *Phys. Rev.* B **50** 17659
[46] Costa-Krämer J L, García N and Olin H 1997 *Phys. Rev. Lett.* **78** 4990
[47] Rodrigo J G, García-Martín A, Sáenz J J and Vieira S 2002 *Phys. Rev. Lett.* **88** 246801
[48] Heurich J, Pauly F, Cuevas J C, Wenzel W and Schön G 2002 *Preprint* cond-mat/0211635
[49] Smit R H M *et al* 2002 *Nature* **419** 906
[50] Reed M A *et al* 1997 *Science* **278** 252
[51] Kergueris C *et al* 1999 *Phys. Rev.* B **59** 12505
[52] Reichert J *et al* 2002 *Phys. Rev. Lett.* **88** 176804
[53] Robertson W M *et al* 1992 *Phys. Rev. Lett.* **68** 2023
Kraus T F *et al* 1996 *Nature* **383** 699
[54] Sánchez-Pérez J V *et al* 1998 *Phys. Rev. Lett.* **80** 5325
[55] Tour J M, Kozaki M and Seminario J M 2001 *J. Am. Chem. Soc.* **120** 8486
[56] Hay P J and Wadt W R 1985 *J. Chem. Phys.* **82** 299
[57] Becke A D 1993 *J. Chem. Phys.* **98** 5648
[58] Taylor J, Brandbyge M and Stokbro K 2002 *Phys. Rev. Lett.* **89** 138301